GIS를 기반으로 한 CT-2 서비스 영역 예측 및 셀설계 시뮬레이터 개발

임 종 수† · 이 봉 석†† · 이 문 수†††

요 약

본 논문에서는 서비스반경이 비교적 짧은 마이크로셀 이동무선채널 환경에서 가입자에게 양호한 통화품질을 제공하기 위한 서비스 영역을 컴퓨터를 이용하여 예측할 경우, 건물과 도로 등의 디지털지도정보를 처리하기 위한 디지털 지도처리 기법 및 현재 운용상에 있는 시스템 PCS, 또는 CT-2 등의 시스템에 셀치국목적으로 활용할 경우에 필요한 요소기술인 전파 전파경로 해석 알고리즘을 제시하고자 한다. 건물이 밀집된 대도시 마이크로셀 무선환경에서의 전파전파경로 해석에 자주 적용되는 광선추적(Ray Tracing) 방식을 실시간으로 처리가 가능하도록 개선된 본 알고리즘은 대상지역의 벡터지도데이터를 closed poly lines 형태 즉, 하나의 폴리곤으로 처리하여 전파손실계산점과 건물차단량에 따른 전파손실량을 분석 예측한다. 본 알고리즘을 적용하여 전파예측분석된 결과와 실측치를 비교하였을 때 5dB 이하의 RMS 오차를 갖는다는 것을 확인할 수 있다.

Development of a Simulator for CT-2 Coverage Prediction and Cell Planning by GIS-Based Approach

Jong-Soo Lim† · Bong-Seok Lee†† · Mun-Soo Lee†††

ABSTRACT

A new design procedure for micro cellular coverage prediction is presented here on this paper, which contains a new propagation analysis algorithm based on processing of vector data representing roads and buildings which mainly affect the propagation phenomena in micro-cell environments. The propagation analysis algorithm presented here has been developed to aim at the practical application for micro-cellular systems such as PCS or CT-2. As all the vectors used here are of closed poly lines, i.e., polygons, a simplified ray path search technique can be developed not only to determine if the calculation points are on the road polygons and but also to calculate the amount of blockage by buildings. The result shows a capability of predicting path loss with an RMS error of 5dB or lower.

1. Introduction

1.1 Microcellular mobile network and its characteristics

Microcells are a viable economic alternative to provide coverage in congested urban areas where rough RF environments limit the coverage size of the ordinary macrocells. Most cellular systems currently use macrocells[1], which are formed in cities by siting the base station antennas on the top of tall buildings. One of the major characteristics of microcell is to utilize the electromagnetic shielding

† 정 회 원 : 한국전자통신연구원 전파지원팀 선임연구원
†† 정 회 원 : 한국통신기술(주) NI 사업부장
††† 정 회 원 : 경상대학교 전자공학과 교수
논문접수 : 1998년 8월 27일, 심사완료 : 1999년 3월 4일

offered by buildings, i.e., small cells whose shapes are determined by the cross sectional area of the buildings and the topography of the roads. Microcell has a coverage formed along the road envelopes like fish-bone[2].

1.2 Microcellular propagation analysis algorithms with a reduction of complexity

Most recent work[3,4] related to microcell propagation prediction has focused mainly on the accuracy of point-to-point prediction by theoretically deterministic models such as ray tracing. When we use such models for the purpose of cell planning, too much time as well as complexity of computation algorithm should be considered to predict path loss for the coverage. Generally, the theoretical models have not been developed in practical application's point of view. In this paper, we present an algorithm with statistical models, where the propagation paths are recognized by using an image processing[6].

Two kinds of propagation prediction models which take respectively different actions for the digitized vector data are included in the algorithm presented in this paper. The selection of models depends on the location of transmitter's antenna. If we place the antenna with a lamp-post level on the public telephone booth, we extract the nodes from the digital map data, which form polygons and links between them in combination with lines and then we focus on the analysis of the propagation prediction along the links between the nodes. Otherwise, we will focus on the blockage of propagation by the buildings. These models are described in more detail in section 2 and 3. Prediction results compared with measurements are given in Section 3.

1.3 Vector data processing based on the digital map for Propagation Prediction

The prediction model presented in this paper requires two-dimensional layout of the urban area by means of vectors describing the building walls and the road blocks. Therefore, we tried a vectorization of a 1:5,000 city map with a very precise information about the buildings and roads in the target area because the map was made from aerial photos. Vectorized objects are expected to have nearly the same width as the real ones.

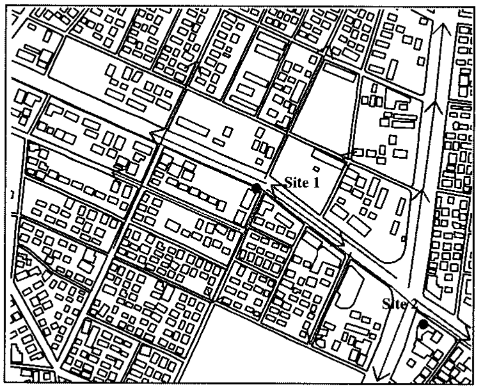

(Fig. 1) Map comprised of buildings and road polygons over a highly populated area in Seoul (arrows : measuremt paths)

(Fig. 1) shows the two dimensional view of a downtown area in Seoul with the street and building data, a good example of a congested urban city. Computer programs have been written to accommodate any commercial geographic data. The prediction model is able to use grid data as well as vector data. If available, terrain height information is stored in a grid format with the comparable resolution to each building size. a×a like the building grid data base.

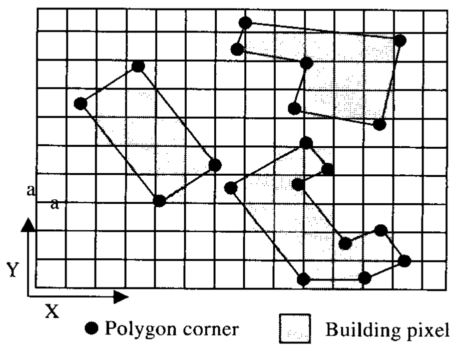

(Fig. 2) Pixel and Vector oriented(building shape lines) building data

The grey marked pixel represent buildings, while the actual building shapes are more accurately described by closed polygon; latter one is called building vector data base. Absolute roof-top height with respect to sea level and building category are assigned to each polygon. Information about interior building details, for instance, walls, doors, furniture, etc. are usually not available. To include effects of interior building structures, assumptions have to be made concerning categories as used for indoor coverage prediction. For the purpose of practical application, some GIS related computer programs have been written to accommodate any commercial geographic data.

2. Simulator Design Architecture And Processing Algorithm

Currently, there are no proven methods and procedures for how accurately building data should be constructed and for how much detailed information it should give for the purpose of microcellular radio network planning. The accuracy of the prediction can not be increased by simply using highly accurate building data because the propagation model itself has a limited accuracy due to highly dependency on the environment, but the computational cost increases with the complexity of the building data.

We shall show the information in the (Fig. 1) will be presumably sufficient for the aforementioned application in section 1.2. The envelopes for roads and buildings are described very well in the vectorized map where each polygon for buildings is completely closed with multiple sides but, isn't for roads. Therefore such information should be generalized or simplified before being put into use. When omni-directional antenna at lamp-post level is placed on an avenue, the propagation mode falls into three categories, i.e., LOS, NLOS and transition region. In microcellular radio channels, there are many corners around a city block. In these heavily shadowed environments, diffraction can be a significant contributor to the received signal strength. Therefore, the transition region can be assumed to be linearly dependent on the angle between LOS and NLOS streets. The above cell type is well known as a fish-bone one.

The following assumptions are made in the algorithm for this prediction model. i) Contiguous buildings infinite in height are located on either side of the roads, Therefore, no account is made for roof-top diffraction. ii) Signal energy through building walls from one street to any other street is negligible, i.e. propagation is solely due to a ducting effect along the street canyon. iii) The underlying terrain is flat. iv) As mentioned before, the propagation loss between adjacent streets depends on the angle subtended. It is assumed that this loss varies linearly with the transition region.

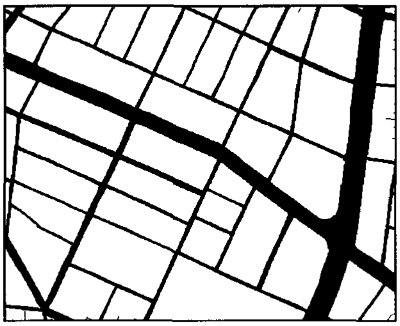

(Fig. 3-1) A polygon filled with black pixels

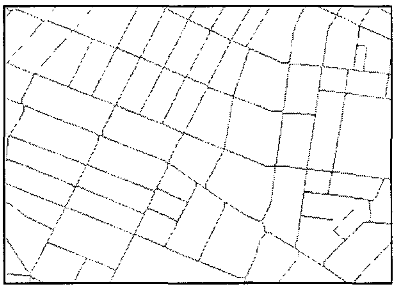

(Fig. 3-2) A thinned raster data

Steps taken in the algorithm for finding the analysis nodes and links are summarized as follows : i) to define boundaries for buildings and roads and to generate only one polygon, where many small polygons enclosing the building blocks are included. ii) to define the nodes as centers on the intersections of streets. iii) to change the colors of pixels that lie within specified regions, i.e. to fill the polygon with a specific color. iv) to convert the vector polygon area into a raster data, as shown in (Fig. 3-1). The action will only affect data in areas lying inside the boundaries of the polygon. v) to thin the raster data by the conditional mark algorithm as follows : the center pixel X and the conditional marks in a 3×3 neighborhood centered about X are examined to create an output pixel(on or off value).

$$G(i,j) = X(i,j) \cap [\overline{M} \cup P(M, M_0, \Lambda, M_7)] \quad (1)$$

where $G(i,j)$ is an output value at (i,j)th pixel and $P(M, M_0, \Lambda, M_7)$ is a conditional mark pattern[6,7]. vi) to find nodes which satisfy the following conditions,

case1) branch off : $$\sum_{k=-1}^{1} \sum_{m=-1}^{1} X(x+k, y+m) \geq 3 \quad (2)$$

case2) non branch off: to use iterative endpoint fit and split algorithm which identifies all locations that have sufficiently high curvature and that are enclosed by subsequences that can fit different straight lines or curves.

vii) to extract links between nodes by using a nearest-neighbor pixel pattern.

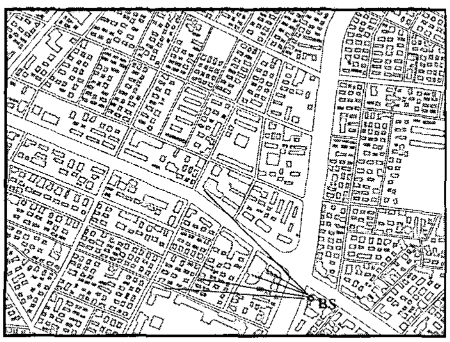

(Fig. 4) Signal prediction by building blockage loss

When omni-directional antenna is placed on the top of buildings with low height (Fig. 4), the signal arriving at the mobile unit is blocked by the individual buildings which weaken the signal strength and is considered as part of the pathloss. Therefore we have to take another approach in our prediction. Our program calculates the path loss based only on the building blockage. The steps for pathloss prediction are as follows : i) Under LOS condition, to calculate the path loss at the mobile site, ii) to calculating the total blockage length by adding the individual building blocks, iii) to find the additional signal attenuation due to the portion of building blocks over the direct path, iv) to add the signal attenuation to the LOS path loss.

(Fig. 5) shows a flow chart for the algorithm, where one of two modes for propagation analysis is automatically selected according to the location of base station as well as the results of the fidelity test of vector data.

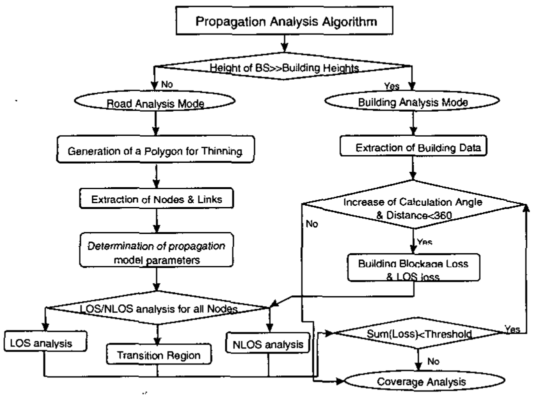

(Fig. 5) Propagation analysis algorithm for microcell design

3. Prediction Model And Measurements Analysis

The selection of models for propagation prediction depends on the location of transmitter's antenna. If we place the antenna with a lamp-post level on the public telephone booth, we focus on the analysis of the propagation prediction along the links between the nodes, i.e. the road analysis mode. Otherwise, we will focus on the blockage of propagation by the buildings, i.e. building blockage analysis mode. Since the ground incident angles of the waves are, in general, small due to the low antenna heights used in small cells, the exact height of buildings in the middle of the propagation paths is not important[3]. Therefore, we can use the vector maps described in the following section to calculate the proportional length of the direct-wave path due to the building blocks.

3.1 Road data analysis mode

The prediction model in the algorithm is an empirical model which is derived directly from measurement data through regression analysis and therefore implicitly accounts for all environmental influences. We stated that the propagation analysis in this mode falls into three categories, i.e., LOS, NLOS and transition region.

The loss formula at each region is described in the following. Each propagation mechanism is treated separately, and the total field is determined via superposition of the individual contributions from each path. Eq.(3). integrates the propagation losses over the n-th linked path over which d_{total} represents a total length and $d_{nHT-corner}$ is a path length to the first transition region.

$$L_{nTH}(d_{nTH-corner}, d_i) = L_{los}(d_{nTH-corner}) \times \prod_{i=1}^{k_{th}} L_{nlos}(d_i) \qquad (3)$$

$$d_{total} = d_{nTH-corner} + \sum_{i=1}^{k_{th}} d_i \qquad (4)$$

Eq.(5). represents the regression model for each path between nodes, d_i are the distances for the different NLOS path along the streets. $\alpha_{nlos(i)}$, $\beta_{nlos(i)}$ are the path loss factors derived from the measurement.

$$L_{nlos(i)}(d_i)[dB] = \alpha_{nlos(i)} + \beta_{nlos(i)} \cdot \log(d_i) \qquad (5)$$

Over a short distance after turning around a corner, there is a sharp increase in propagation loss on the order of 20~30dB. Even though this distance is typically less than 20 m, the attenuation in this region has been described as a linear function of angle subtended as shown in Eq.(6). Which formula should be applied to the next path depends of the angle subtended. CL_{max} is determined from the measurement.

$$L_{nlos}(d_i)[dB] = \begin{cases} CL_i(d_i(\theta)) \ldots\ldots\ldots\ldots\ldots\ldots d < d_i(\theta)_m \\ CL_{max} + \alpha_{nlos} + \beta_{nlos}\log(d_i) \ldots d > d_i(\theta)_n \end{cases} \qquad (6)$$

$$d_i(\theta)_{max} = k \cdot [\theta] \ldots \theta_x \le \theta \le \theta_\delta$$

$$CL_{max} : defined$$

(Fig. 6) shows the measurement data over roads crossing a main LOS street where a transmitter is placed. A sharp drop in signal strength may happen over a very short distance in this transition region on either side of streets.

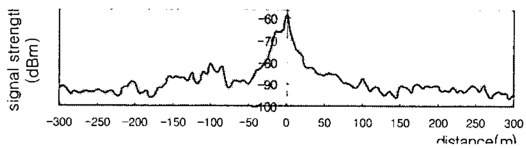

(Fig. 6) Corner loss from a LOS into either side of streets

Signals from more than one path would contribute to the received signal strength. The resultant signal would be the vector sum of the contributions. However, using the model adopted in the algorithm, the signal energy received at Rx is defined by the best serving effective virtual source.

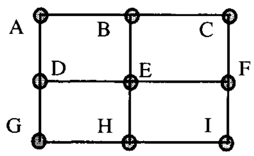

(Fig. 7) Nodes and Links between A and Inodes

Therefore the algorithm establishes one path out of a large number of plausible paths along the links between Tx and Rx when dramatic reduction of calculation time is needed for system design by using a great number of sites(ex] approximately 100 sites in one district area).

The following process shows an instance to find the path between A and I nodes as shown in (Fig. 7). i) to find LOS nodes from node A in all directions for adjacent nodes linked each other. ii) to store the nodes into stack. iii) after moving virtual source points to the nodes in stack, to repeat the same procedure as in i)~ii) until the paths reach i-th node or signal strength comes to a pre-defined threshold level.

step 1) A→D & G nodes
A→B & C nodes
step 2) D→E & F nodes
G→H & I nodes : candidate1
B→E & H nodes
C→F & I nodes : candidate2
step 3) E→B & D & F & H nodes
F→C & E & I nodes : candidate3
H→G & I nodes : candidate4

(Fig. 8) An instance process to find a path from A to I node

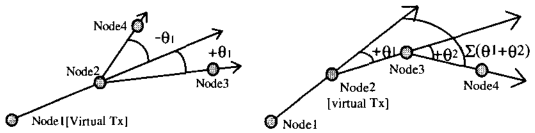

(Fig. 9) Decision of LOS/NLOS by the angles subtended between nodes

The algorithm sets a transmitter position as an origin to determine whether or not the very next link of a node is LOS and then compares the deviation from the just previous path with a threshold. Final decision depends on the angle accumulated up to the start node which belongs to the road for mode selection. The accumulation might result in making all the links NLOS modes although the adjacent ones have little deviation from each other. To avoid such a result, the algorithm establishes the virtual transmitter on the nodes and moves the origin to the next node along the links.

3.2 Building analysis mode

In this mode, it is important to find the additional signal attenuation by the building blockage. The additional signal attenuation curve (α_B) based on the building blockage (B) was found experimentally.

$$\alpha_B(B) = L_{nlos}(d) - L_{los}(d), \quad B = \sum_{i=1}^{n} a_i \qquad (6)$$

where a_i represents individual building blocks.

$$L_{los}(d) = L_0 + 10 \cdot n_{los} \cdot \log(d) \qquad (7)$$

The coefficients in Eq.7 are derived from the measurements for LOS conditions.

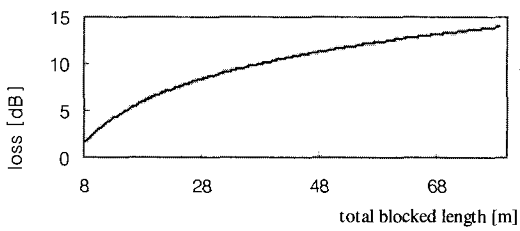

(Fig. 10) Additional loss by blockage

The following equation describes the Lee model for a micro-cell, and the (Fig. 10) represents an additional signal attenuation curve, where transmitted power and height-effect of the antenna are considered as P_t and A_{eff} respectively[4].

$$P_{los} = \begin{cases} P_t - 77(dBm) - 21.5 \cdot \log(\frac{d}{31}) + \\ \quad A_{eff} \ldots 31 \le d(m) \langle 61 \\ p_t - 83.5(dBm) - 14 \cdot \log(\frac{d}{61}) + \\ \quad A_{eff} \ldots 61 \le d(m) \langle 610 \\ P_t - 93.3(dBm) - 36.5 \cdot \log(\frac{d}{610}) + \\ \quad A_{eff} \ldots 610 \le d(m) \langle 1500 \end{cases} \qquad (8)$$

3.3 Measurements and analysis

Accurate knowledge of path loss is necessary for wireless system design. When measured data are unavailable, designers typically rely on statistical models to predict the path loss incurred over urban mobile radio channels.

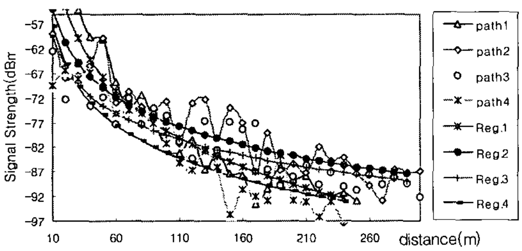

(Fig. 11) Linear Regression Analysis over Specific Paths

As we shall see, the model parameters derived from the measurements for path loss on some typical CT-2 propagation environments are highly dependent on the propagation environments. Many measurements with the receiving antennas placed at intervals of 10 m along the pavements were performed. Transmitter with an 5dBi omni antenna operating at a carrier frequency of 912MHz produces an output power of 10mW.

(Fig. 11) shows the linear regression analysis for the measurement data over all the paths at the highly populated area (Fig. 1) in Seoul, where the signal was beyond the pre-defined threshold level for receiver unit's sensitivity.

<Table 1> shows the regression analysis for measurement data, which were gathered along roads around transmitters in the area sketched in (Fig. 1). Resultant parameters are used to fit the LOS and NLOS equations for the road mode in the simulator. In other words, coefficients depending upon the environments have applied to the model in a fishbone environment in the algorithm. (Fig. 12) shows the measurement data for the building blockage loss when the base station is well below the roof tops of the adjacent buildings.

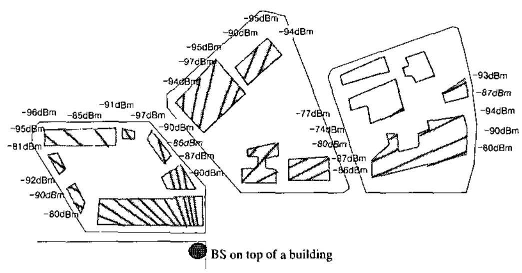

(Fig.12) Measurement data for the building blockage loss

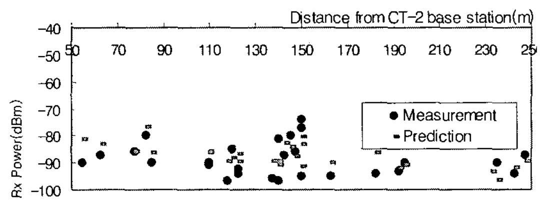

(Fig. 13) Comparision between measurement and prediction by building blockage

〈Table 1〉 Result of the regression analysis over specific regions

Streets around site1					Streets around site2				
Path	# of Points	Coefficients.		Error (SD)dB	Path	# of Points	Coefficients		Error (SD)dB
		α	β				α	β	
1(NLOS)	25	127.68	-36.17	3.97	1(NLOS)	21	102.23	-26.18	3.828
2(LOS)	37	103.00	-22.96	3.83	2(NLOS)	19	110.61	-31.24	4.760
3(LOS)	37	94.570	-20.06	3.32	3(LOS)	28	107.33	-26.55	4.952
4(LOS)	24	102.43	-25.80	4.72	4(LOS)	27	97.348	-22.71	2.943
5(LOS)	29	90.835	-20.00	5.56	5(LOS)	14	108.34	-29.67	3.100
6(LOS)	26	86.589	-17.85	3.61	6(LOS)	16	99.175	-24.0	5.928
7(LOS)	25	103.84	-26.12	3.21	7(LOS)	22	100.89	-22.72	2.829

〈Table 2〉 Prediction of the building blockage loss over specific building block

MEASUREMENT POINTS	RECEIVED POWER	BLOCKED LENGTH	LOS STRENGTH	BLOCKAGE LOSS	PREDICTED VALUE	ERROR
147m	-86dBm	30m	-79.0dBm	8.65dB	-87.7dBm	1.7dB
142m	-87dBm	12m	-78.8dBm	3.90dB	-82.7dBm	4.2dB
145m	-80dBm	15m	-78.9dBm	4.89dB	-83.8dBm	3.8dB
195m	-90dBm	37m	-80.8dBm	9.86dB	-90.6dBm	0.6dB
162m	-95dBm	40m	-79.6dBm	10.2dB	-89.8dBm	dB

4. Computational Results And Application System

The following (Fig. 14) shows a result of propagation prediction for CT-2 system over a downtown in Seoul. The coverage areas are indicated by the shaded region. We can find two different coverage appearances as described in section II. Circles on the maps represent the locations of the base stations. The simulator has some functions to control transparency and display level for the coverage in the building analysis mode. Therefore, we can easily find buildings and roads which affect the shape of the coverage. In the road analysis mode, the simulator performs calculation along the roads as propagation paths and also limits the coverage analysis region into roads. Although a circular cell approximation for determination of the maximum cell radius based on an LOS model provides an estimate for the length of a coverage region, the (Fig. 14) shows that it cannot be applied to the microcell case. As it looks here, the propagation in micro-cells is essentially determined by the topology of the streets and buildings, and therefore the shapes of microcells are irregular depending on propagation environments.

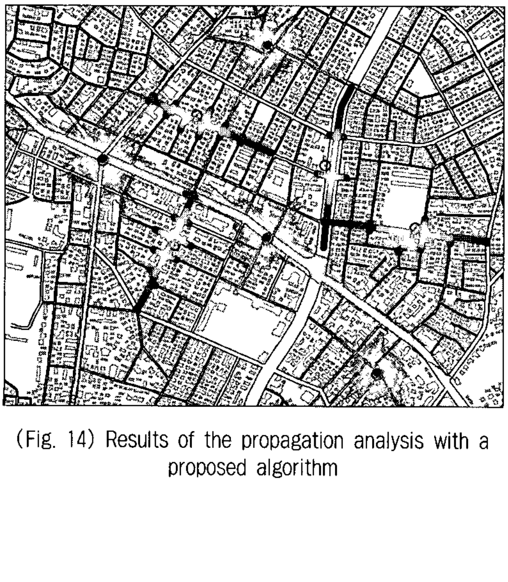

(Fig. 14) Results of the propagation analysis with a proposed algorithm

5. Conclusion And Comments

When engineers design cell sites, it is necessary to use morphology, antenna, communication system, subscriber information and etc. Especially in microcell design, we should focus upon processing of GIS data as well as propagation prediction algorithm for more accurate propagation analysis. Though we can get more accurate results when ray theoretic methods such as a ray tracing technique are applied for the prediction, it costs us too much to construct GIS data with respect to individual building heights and e.t.c. and it also takes us so much time to get the final results due to its relative complexity in calculation algorithm when compared with the proposed method. Especially, in case that there are many sites for CT-2 service to cover the entire service area with due to its small coverage, we face the practical problems like the expense and the time mentioned above. A modified fish-bone model presented here is fitted by the values extracted from the measurement data and uses 2-dim. data instead of 3-dim. to solve the problems and then it has become possible to predict the propagation in real time. A new prediction algorithm based on two dimensional building data has been developed, which can be used for mobile communication system design. The simulation result shows the validity of the simulator with an rms error of 5dB or lower, although it doesn't use sophisticated ray-theoretic methods such as ray tracing. If some correction factors are included in the algorithm, it is expected that the more accurate result can be obtained.

References

[1] The Development of Korean Wave Propagation Model in Pager System by ETRI, pp.165-185, 1995.

[2] M. J. Feuerstein, "Path Loss, Delay Spread, and Outage Models as Functions of Antenna Height for Microcellular System Design," IEEE Transaction on Vehicular Technology, Vol.43, No.3, pp.487-497, Aug., 1994.

[3] Parsons, J.D.,Turkmani, A.M.D., and Khorami, M., "Microcellular radio propagation modelling." OEE 6th Int'l. Conf. On Mobile Radio and Personal Communications, Published, No.351, Dec., 1991, pp.182-190.

[4] Turkmani, A.M.D., and Arowojolu, A.A., "Prediction of microcellular radio propagation characteristics using ray theory," IEE Colloquium on Microcellular Propagation Modelling, Savoy Place, London, 5th Nov., 1992, pp.2/1-2/6.

[5] Scott Y. Seidel, "Research in Site Specific Propagation Modeling for PCS System Design," IEEE 43th Vehicular Technology Conference. Vol.2, pp.261-264, 1993.

[6] W. C. Y. Lee, "Lee's Model," IEEE 42th Vehicular Technology Conference. pp.343-348, 1992.

[7] William K. Pratt, "Shrink, Thin and Skeletonized Conditional Mark Patterns," in Digital Image Processing 2nd Edition, John Wiley & Sons, pp. 461-473, 1991.

[8] R. O. Duda and P. E. Hart., Pattern Classification and Scene Analysis, Wiley-Interscience, New York, 1973.

임 종 수

e-mail : ljten@etri.re.kr

1988년 경북대학교 전자공학과(공학사)

1990년 경북대학교 정보통신공학과(공학석사)

1990년~1995년 SK Telecom 중앙연구소 선임연구원

1996년~1998년 한국통신기술(주) 연구소 무선기술팀 과장

1999년~현재 한국전자통신연구원 전파자원팀 선임연구원

관심분야 : 이동통신, 마이크로파, 기지국 체적화 등

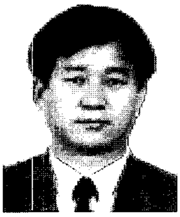

이 봉 석

e-mail : silvest@kti.co.kr

1980년 광운대학교 통신공학과(공학사)

1991년 경희대학교 산업정보대학원 전자공학과(공학석사)

1997년~현재 경상대학교 대학원 전자공학과(박사과정)

1980년~1982년 동아건설산업(주) 통신주임

1983년~1986년 Ericsson System Manager

1986년~현재 한국통신기술(주) NI 사업부장

관심분야 : 이동통신, 마이크로파, 안테나, GIS 등

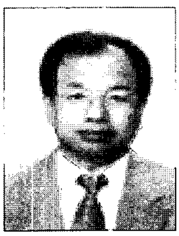

이 문 수

e-mail : munslee@nongae.gsnu.ac.kr

1970년 2월 한국항공대학교 통신공학과 졸업

1984년 8월 한양대학교 대학원 전자통신과(공학박사)

1981년 3월~1986년 3월 제주대학교 부교수

1986년 9월~1987년 8월 미국COMSAT 연구소 연구원

1986년 3월~현재 경상대학교 전자공학과 교수

1997년 9월~현재 경상대학교 부설 정보통신연구센타 소장

관심분야 : 이동통신, 마이크로파, 안테나, GIS 등